Impact of fish protein concentrate on apparent viscosity and physical properties of soy protein concentrate subjected to thermomechanical treatment

Rafiq Ahmad[a], Åge Oterhals[b], Ying Xue[c], Tore Skodvin[d], Tor Andreas Samuelsen[b,*]

[a] Cargill, Dirdalsstranda 51, N-4335, Dirdal, Norway
[b] Nofima, P.O. Box 1425 Oasen, N-5844, Bergen, Norway
[c] Department of Clinical Dentistry, University of Bergen, Årstadveien 19, N-5009, Bergen, Norway
[d] Department of Chemistry, University of Bergen, Allégaten. 41, N-5007, Bergen, Norway

ABSTRACT

The aim of this research was to investigate the plasticizing and binding effect of fish protein concentrate (FPC) on soy protein concentrate (SPC) with the use of a capillary rheometer with pre-shearing capabilities. A 3-component mixture design was used to study the effect of the variables SPC, FPC and water. Mixture models with R^2 in the range of 0.703–0.998 (P < 0.01) were established for apparent viscosity, extrudate hardness and expansion parameters of the plasticized materials. Extrudate microstructure as porosity, pore size distribution, cell wall thickness and distribution, were measured with the use of X-ray microtomography and models established with R^2 in the range of 0.582–0.941 (P < 0.02). The mixture components affected apparent viscosity with the highest value observed for the blend with maximum SPC concentration (1381.6 Pa s) followed by maximum FPC concentration (858.6 Pa s), and lowest for the blend with maximum water concentration (398.0 Pa s). Lowest pellet hardness (136.2 N), density (904.3 kg/m³) and highest expansion (1.44) were found for the blend with maximum SPC concentration and can be attributed to incomplete thermomechanical transformation. Extrudate physical properties and expansion were explained by the extrudate microstructure. FPC added at a concentration of 65–70 g/kg gave values of hardness, extrudate density and microstructure similar to SPC added 100 g/kg of water, confirming the potential for the use of FPC as plasticizer and binder in the fish feed extrusion process.

1. Introduction

The fish feed extrusion process is a thermomechanical process that transforms the feed ingredients into a plasticized and high viscous flowable material that is shaped through dies, cut into pellets, dried and added oil in a vacuum coating operation. The durability of the final product and expansion parameters are controlled by moisture and high temperature achieved by steam injection and viscous heat dissipation. The performance of the process is influenced by the physicochemical, thermal and rheological properties of the feed ingredients and type and concentration of added plasticizer. The feed must have sufficient expansion to meet target oil adsorption and high durability to withstand bulk transport and pneumatic feeding (Sørensen, 2012). The pellet size,

fat content and physical quality characteristics will vary depending on the growth phase of the fish.

The use of fishmeal in salmon feed formulations has been reduced from 65% to 18% in the last two decades and has partly been replaced by alternative plant-based ingredients as soy protein concentrate (SPC), vital wheat gluten (WG) and sunflower meal (SFM). WG has high protein content (> 80%), however, an unbalanced amino acid profile and reduced oil adsorption, caused by change in pellet microstructure, restrict the use. SFM has low protein content and is high in fiber and non-starch polysaccharides which limits the use due to nutritional constraints. SPC is the dominant plant protein ingredient, replacing approximate 21% of the fishmeal. This is possible due to its high protein content, balanced amino acid profile and low carbohydrate and fiber

contents (Sørensen et al., 2011; Draganovic et al., 2013; Ytrestøyl et al., 2015).

Compared to fish meal and other plant proteins, SPC demands high moisture level and temperature in the extrusion process to obtain a satisfactory plasticization and durable pellets (Bengoechea et al., 2007; Draganovic et al., 2011; Oterhals and Samuelsen, 2015; Ahmad et al., 2018; Samuelsen et al., 2018). This give the feed manufacturing industry challenges related to pellet quality and drying costs. The use of alternative plasticizers to partly replace water can reduce extrudate moisture content and energy requirements in the dryer and improve physical feed quality. Oterhals and Samuelsen (2015) studied the plasticization effect of water solubles (water-soluble dry matter; WSDM) in fishmeal by use of a closed-chamber capillary rheometer (Strahm et al., 2000). Within the moisture range of 85–223 g/kg a significant effect on reduced glass transition (T_g) and flow-starting (T_f) temperature with increased addition of WSDM from 95 to 380 g/kg DM were observed. The main effect on T_g and T_f were 3.1 and 1.2 times higher, respectively, for moisture compared to WSDM. The plasticizing effect of WSDM could be attributed to the content of free amino acids, peptides and N-containing putrefaction products. Ahmad et al. (2018) confirmed the plasticization effect of the amino acid proline on SPC within the moisture and proline range of 163–245 g/kg and 0–100 g/kg DM, respectively. In the study, moisture was 2.2 and 1.3 times more effective compared to proline on T_g and T_f, respectively. In industrial manufacturing practice, any protein hydrolysate with a high degree of hydrolyzation may be used as a cost-effective solution. The apparent viscosity at T_f was defined by the capillary die geometry and applied pressure and measured to 10^5 Pa s (Oterhals and Samuelsen, 2015; Ahmad et al., 2018). The observed difference between T_f and T_g reflects the temperature increase required to reduce the viscosity of the material from 10^{12} Pa s at T_g to the critical flow level of 10^5 Pa s at T_f. A material with high T_f - T_g requires higher temperature increase to reach this critical value. The large variation in T_f - T_g (36–149 °C and 103–162 °C for the WSDM/moisture and proline/moisture system, respectively) indicates a significant effect of the studied plasticizers on the viscosity reduction of temperature increase in the rubbery phase.

There is an increasing interest in the use of fish protein concentrate (FPC) in salmon diets. FPC is produced from fish offcuts and offal from filleting, gutting and other fish processing operations and is therefore a sustainable, environmentally friendly alternative protein ingredient. The raw material is minced and added formic acid to reduce the pH ≤ 4. This gives optimal conditions for protein hydrolysis by the fish pepsin and a microbiological stable product. The hydrolyzed crude fish silage is heated and processed over a 3-phase decanter centrifuge to remove oil and residual particulate matter before concentrated to an FPC with a dry matter of 40–50% (Sikorski et al., 1995). FPC may have a plasticizing and binding effect similar to what has been documented for fish solubles and proline added to fishmeal and SPC (Oterhals and Samuelsen, 2015; Ahmad et al., 2018). To our knowledge no studies have documented this effect of FPC in SPC rich diets.

Capillary rheometry is a common technique used to study rheological behavior of protein and starch formulations; however, ordinary capillary rheometers do not apply mechanical shearing prior to the capillary die like in extrusion processing (Nunez et al., 2010). In a newly developed pre-shearing capillary rheometer, RheoArt (AR-Technologies, Aydat, France), mechanical treatment can be performed in a conical shear cell to produce a rubbery mass prior to viscosity measurements through a capillary die. RheoArt is a more advanced and improved version of RheoPlast (Vergnes and Villemaire, 1987) which has been reported to give results comparable to the extrusion process (Vergnes and Villemaire, 1987; Barron et al., 2000; Nunez et al., 2010). The new RheoArt can be a cost-effective analytical tool and test system enabling to simulate conditions in the fish feed extrusion process.

The impact of process conditions and feed ingredients on physical feed quality and expansion parameters have been studied in detail (Glencross et al., 2010; Kraugerud et al., 2011; Draganovic et al., 2011,

2013; Samuelsen and Oterhals, 2016; Dethlefsen, 2017; Samuelsen et al., 2018). However, less effort has been used to study the microstructure induced by these variations. X-ray microtomography has been applied to study the microstructure properties of starch-based extrudates (Trater et al., 2005; Agbisit et al., 2007; Robin et al., 2010) and extruded fish feeds (Draganovic et al., 2013; Dethlefsen, 2017). However, to our knowledge there is a lack of information regarding the use of X-ray microtomography to evaluate change in microstructure of feed blends added different type and concentration of plasticizers.

The objectives of this study were to (i) assess the plasticizing and binding effect of FPC and water concentrations in a high SPC feed composition using the RheoArt, (ii) study apparent viscosity of the rubbery SPC blends, and (iii) evaluate physical quality, expansion parameters and microstructure development of the produced extrudates. The results are discussed within the context of fish feed extrusion but will also be of general relevance for the processing of food and bioplastic formulations.

2. Materials and methods

2.1. Materials

Soy protein concentrate (SPC) was obtained from Sementes Selecta (Goiania, Brazil) and vital wheat gluten (WG) from Tereos Syral (Aalst, Belgium). Whole wheat flour, of bakery quality (Wheat; falling number > 200 s), was purchased from Norgesmøllene AS (Vaksdal, Norway). LT-quality Fishmeal (FM) was obtained from Norsildmel AS (Bergen, Norway) and fish protein concentrate (FPC) from Aquarius AS (Lovund, Norway). Proximate chemical composition of the ingredients and experimental feed mixes are given in Tables 1 and 2, respectively. Soy lecithin was obtained from Denofa AS (Fredrikstad, Norway) and food grade sunflower oil was purchased locally.

2.2. Experimental design and sample preparation

A 3-component simplex-centroid mixture design (Cornell, 2011) was applied to quantify the influence of mixture variables SPC, FPC and water on the studied responses (Tables 3 and 4). Eleven experimental samples were prepared. Due to the different fat content in the ingredients, the SPC and FPC concentrations were based on fat free dry matter (FFDM) and thereafter standardized to equal amount of fat by adding sunflower oil. Since fat is a lubricator this was performed to remove fat content as a variable in the design. Within the mixture design space, SPC was varied between 354.7 and 454.7 g FFDM/kg, FPC between 0 and 100 g FFDM/kg and water between 200 and 300 g/kg. The design represents a triangle with a total of 7 experiments (EX1 to EX7) including three vertex points (maximum concentration of corresponding mixture variable), three edge points located at the mid-way of two corresponding vertex points (equal combination of corresponding

Table 1
Proximate chemical composition of the ingredients (g/kg).

Components	FM	WG	Wheat	SPC	FPC
DM	914	949	879	938	426
In DM					
Crude protein	721	851	149	651	716
Water-soluble protein	128	71	8	74	665[a]
Fat	138	80	26	28	73
Ash	161	8	14	67	124
Salt (NaCl)	43	1	2	1	49
Starch	–	95	646	14	–

DM, Dry matter; FM, fishmeal; FPC, fish protein concentrate; SPC, soy protein concentrate; WG, vital wheat gluten; Wheat, whole wheat flour.

[a] Water-soluble protein fractions: Molecular weight 1000-500 Da, 8.2%; Molecular weight 500-200 Da, 19.9%; Molecular weight < 200 Da, 61.4%.

Table 2
Formulation and chemical composition of the experimental feed mixes (g kg^{-1}).

	EX1	EX2	EX3	EX4	EX5	EX6	EX7
SPC	498.6	388.9	388.9	443.8	388.9	443.8	425.5
FPC	0.0	253.2	0.0	126.6	126.6	0.0	84.4
Added water	138.5	0.0	245.3	69.2	122.6	191.9	127.9
FM	126.6	126.6	126.6	126.6	126.6	126.6	126.6
WG	114.5	114.5	114.5	114.5	114.5	114.5	114.5
Wheat	116.8	116.8	116.8	116.8	116.8	116.8	116.8
Sunflower oil[a]	5.0	0.0	7.8	2.5	3.9	6.4	4.3
Chemical composition[b]							
FFDM	754.7	754.7	654.7	754.7	704.7	704.7	721.4
Fat	45.3	45.3	45.3	45.3	45.3	45.3	45.3
Water	200.0	200.0	300.0	200.0	250.0	250.0	233.3
Crude protein	495.9	506.1	428.9	501.0	467.5	462.4	477.0
Water-soluble protein	58.2	122.2	50.5	90.2	86.4	54.3	77.0
Starch	83.4	82.7	82.0	83.1	82.4	82.7	82.7
Ash	52.3	58.8	45.4	55.6	52.1	48.9	52.2
Salt (NaCl)	5.8	11.0	5.7	8.4	8.3	5.7	7.5

DM, dry matter; EX, experimental feed mixes; FFDM, fat free dry matter; FM, fish meal; FPC, fish protein concentrate; SPC, soy protein concentrate; WG, vital wheat gluten; Wheat, whole wheat flour.

[a] Sun flower oil was added to standardize the experimental feed mixes (EX) with an equal level of 45.3 g/kg fat.
[b] Chemical composition was calculated based on chemical analyses (Table 1) and amount of water and fat (sunflower oil) added.

Table 3
Pseudo and actual units for the experimental design variables.

ENo	Feed mix	Pseudo			Actual		
		SPC	FPC	Water	SPC (g FFDM/kg)	FPC (g FFDM/kg)	Water (g/kg)
1	EX7	0.333	0.333	0.333	388.1	33.3	233.3
2	EX6	0.500	0.000	0.500	404.7	0.0	250.0
3	EX11	0.500	0.500	0.000	404.7	50.0	200.0
4	EX2	0.000	1.000	0.000	354.7	100.0	200.0
5	EX5	0.000	0.500	0.500	354.7	50.0	250.0
6	EX3	0.000	0.000	1.000	354.7	0.0	300.0
7	EX14	0.333	0.333	0.333	388.1	33.3	233.3
8	EX13	0.500	0.000	0.500	404.7	0.0	250.0
9	EX12	0.000	0.500	0.500	354.7	50.0	250.0
10	EX1	1.000	0.000	0.000	454.7	0.0	200.0
11	EX4	0.500	0.500	0.000	404.7	50.0	200.0

ENo, experimental number; EX, experimental feed mix; FFDM, fat free dry matter; FPC, fish protein concentrate; SPC, soy protein concentrate.

two mixture variables) and overall centroid (equal combination of corresponding three mixture variables). EX11, EX12, EX13 and EX14 are true replicates of EX4, EX5, EX6 and EX7, respectively (Table 3). The true replicates will include both sample preparation, experimental and analytical error and used to determine the pure error and lack of fit error. Insignificant lack of fit indicates that the model can be used as a predictor of the response. In addition to the 100 g mixture design contribution, the experimental samples contained 900 g of a fixed base composition consisting of FM (100 g FFDM/kg), WG (100 g FFDM/kg), Wheat (100 g FFDM/kg), SPC (354.7 g FFDM/kg), water (200 g/kg) and fat (45.3 g/kg). The solid powdery ingredients were ground in a Retch SR-3 centrifugal mill (Retsch GmbH, Haan, Germany) with a ring sieve aperture of 0.5 mm and mixed in a DITO SAMA blender (Pordenone, Italy). The water and fat content were standardized by using an emulsion of sunflower oil in the predetermined content of water (Table 3). Lecithin was added to 10% on fat basis to stabilize the emulsion. The predetermined amount of FPC (Table 3) was added together with the emulsion. The samples were conditioned in closed containers at 4–5 °C for 24 h and homogenized in a blender before analysis of moisture content. Average value, based on triplicates, was in the range ± 0.5% of predicted moisture content. The experimental samples were stored in the freezer (- 20 °C) until use.

2.3. Chemical analysis

Crude protein (N x 6.25) in the feed ingredients was analyzed by use of the Kjeldahl method (ISO 5983-2) and water-soluble protein by hot water extraction as described by Oterhals and Samuelsen (2015). The fat content was determined according to Bligh and Dyer (1959). Total ash content was determined according to (ISO 5984) and salt (NaCl) content based on chloride using AOAC (2000) method 937.09. The moisture level in raw materials and experimental samples was analyzed according to ISO 6496. Peptide size distribution for the FPC water-soluble protein fraction was measured by HPLC size exclusion chromatography using a Superdex™ Peptide 10/300 GL (I.D. 10 mm × 300 mm) (GE Healthcare, Upsala, Sweden) column as described by Oterhals and Samuelsen (2015).

2.4. Thermomechanical processing

A newly developed capillary rheometer with pre-shearing capabilities, RheoArt (Fig. 1), was used to plasticize the sample material prior to determination of apparent viscosity, extrudate physical quality and microstructure. The instrument consists of a feeding zone, shearing and extrusion chamber, capillary die and two pistons. The outer feeding piston can move vertically to push and compress the material. The
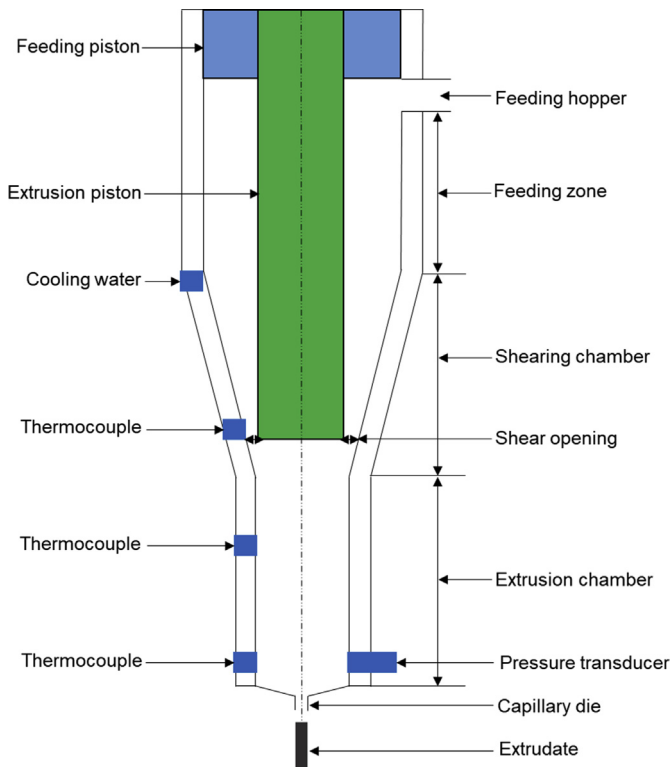
Table 4
Measured response variables.

ENo	Feed mix	Apparent viscosity (Pa s)	Starch gel [a] (%)	Hardness (N)	SEI	Extrudate density (kg m^{-3})	Closed porosity (%)	Open porosity (%)	Total porosity (%)	Solid SV ratio ($\times 10^{-3}$/μm)	MCWT μm	MCS μm	Connectivity density ($\times 10^{-7}$/μm^3)
1	EX7	705.7	88.5	241.0	1.25	983.8	0.48	36.4	39.6	65.6	47.1	136.70	88.9
2	EX6	673.9	91.8	179.2	1.30	942.3	0.25	46.5	46.6	90.0	37.7	132.74	154.4
3	EX11	1023.9	85.5	209.5	1.30	980.5	0.49	41.9	42.1	73.8	42.5	136.60	102.1
4	EX2	858.6	89.1	232.3	1.18	1095.2	0.56	36.2	36.5	53.1	58.0	152.04	76.4
5	EX5	596.3	91.0	225.8	1.15	1027.2	0.79	36.7	37.2	54.1	53.3	141.49	76.9
6	EX3	398.0	92.0	198.6	1.10	1030.7	0.80	42.3	42.8	77.3	36.6	127.65	95.6
7	EX14	705.4	89.7	214.2	1.22	1008.1	0.49	40.5	40.8	66.4	49.0	133.40	83.3
8	EX13	673.0	87.9	170.9	1.30	958.0	0.33	42.7	42.9	78.2	40.5	139.08	99.5
9	EX12	573.5	87.6	244.5	1.13	1055.8	0.54	37.6	37.9	58.7	51.4	143.94	82.8
10	EX1	1381.6	78.5	136.2	1.44	904.3	0.25	51.9	52.0	102.5	33.9	136.42	153.4
11	EX4	1031.2	91.6	194.9	1.30	987.0	0.54	45.1	45.4	70.9	45.4	188.82	89.1

ENo, experimental number; EX, experimental feed mix; MCS, mean cell size; MCWT, mean cell wall thickness; SEI, sectional expansion index; Starch gel, degree of starch gelatinization; SV, surface to volume.
[a] % of total starch.

Fig. 1. Longitudinal section of the RheoArt with conical design.

extrusion piston can rotate to create a shear field in the conical shear cell and can move vertically to push the plasticized material from the extrusion chamber through the capillary die for apparent viscosity measurement. Temperature can be controlled and measured in four zones; initial temperature at shearing chamber inlet by cooling water, in the shearing chamber, and upper and lower part of the extrusion chamber by use of thermocouples (Fig. 1). The material was introduced from the feeding zone and compacted in the shearing chamber under the force of the feeding piston. The temperature in the cooling and heating zones were kept constant at 100, 110, 110 and 110 °C, respectively. The extrusion piston was rotated at pre-determined velocity of 150 rpm to create a shear field and simultaneously the material was pushed and plasticized at a constant speed of 0.15 mm/sec by the feeding piston through a predefined circular shear opening of 1 mm into to the extrusion chamber. The shearing duration was completed when the pressure reached 30 bar at the bottom of extrusion chamber upstream the capillary die (Fig. 1). The feeding piston stops, and the inner piston moves downward at a predetermined speed of 1.172 mm/s to push the material through the capillary die. This equals and apparent wall shear rate at 300 s^{-1} in the capillary die. The shear rate was selected to meet sufficient time for stable and accurate viscosity measurement and to collect the extrudate string. In addition, wall slip was not observed for any of the samples at the selected shear rate. The shear rate is also close to levels normally applied through the extruder die in pilot scale studies (400-600 s^{-1}; Samuelsen et al., 2013, 2018; Samuelsen and Oterhals, 2016). Apparent wall shear stress and viscosity were calculated based on the measured pressure drop, capillary die radius (0.001 m) and capillary die length (0.016 m) as described by Oterhals and Samuelsen (2015). The analyses were run in duplicates and extrudate string of replicate B was collected during the movement of the extrusion piston between the time interval of 5–40 s. Based on the duplicate measurements, the standard deviation of apparent viscosity was estimated to be 9.2 Pa s.

2.5. Extrudate properties

The collected extrudate strings were frozen at −80 °C, cut into pieces at equal length of 15 ± 1 mm using a scalpel and immediately frozen overnight at −80 °C. The frozen extrudates were lyophilized in a HETO FD8 dryer (Heto-Holten, Allerød, Denmark). The dried samples were conditioned against air at ambient temperature in a closed room to equal water activity and stored frozen in closed container until use. Hardness was measured on horizontally placed extrudate pieces using a texture analyzer (TA-HDi; Stable Micro system Ltd, Surrey, UK) as described by Samuelsen and Oterhals (2016). The speed of a load arm was set to 0.5 mm s^{-1} and the penetration distance to 1 mm. Extrudate diameter (d_e) and length (l) were measured using a digital Vernier caliper. Sectional expansion index (SEI) was calculated by dividing the square of the extrudate diameter by the square of the capillary die diameter. Extrudate density (ρ) was calculated based on:

$$\rho = \frac{4\,m}{\pi\,l\,d_e^2} \tag{1}$$

where m is the mass of the extrudate. The extrudate pieces were treated individually and reported values based on the average of 15 analyses. Total starch and degree of starch gelatinization were determined using the glucoamylase method described in Chiang and Johnson (1977) and Samuelsen and Oterhals (2016).

2.6. Extrudate microstructure

Micro-CT scanning (Landis and Keane, 2010) was performed using a desktop X-ray microtomography (XMT) imaging system (SkyScan 1172, Bruker-microCT, Kontich, Belgium). Scanning was set at 40 kV/250 μA with an isotropic resolution of 2.5 μm for each representative piece of sample. Each sample was placed on the rotation stage between source and detector. The detector was used in the 4 × 4 binning mode leading to a pixel resolution of 2.5 μm. With an exposure time of 468 ms, a rotation step of 0.3°, a frame averaging of 4 and an acquisition over 180°, the total scan time was 53 min per sample. The projection images were reconstructed into 2D cross section images using reconstruction software (NRecon v.1.7, Bruker-microCT, Konitch, Belgium). The Feldkamp algorithm was implemented for reconstruction. Smoothing of the projection images prior to reconstruction was done with a value of 2. The ring artifacts were reduced with strength of 8 and the beam hardening correction was set at 26%. The 3D structural analyses were calculated using CTAn v.1.12 software (Bruker-microCT, Kontich, Belgium) with grey threshold of 40. An average diameter of each sample was calculated based on randomly diameter measurement at different layers in CTAn. The 3D analyses were performed on an appropriate volume of interest (VOI). The VOI was set as the average extrudate diameter minus 0.2 mm and 5 mm in height, which were selected from random position of the total scanned height (∼7 mm). The porosity of sample was calculated as the ratio of the volume of the pores to the VOI. A closed pore in 3D is a connected assemblage of space (black) voxels that is fully surrounded on all sides in 3D by solid (grey) voxels. Closed porosity (%) is the volume of closed pores as a percent of closed pore volume within the VOI. Open porosity (%) is the ratio of volume of pores which has any connection in 3D with the space outside the object VOI. Total porosity (%) is the volume of all open plus closed pores as a percent of the total VOI. The structure separation function and the thickness distribution function were used to calculate pore cell size volumetric-distribution and pore cell wall thickness-volumetric distribution, respectively, within the VOI. In addition, the microstructure of sample was also described in terms of mean cell wall thickness (MCWT, μm) and mean cell size (MCS, μm). Connectivity density ($\times 10^{-7}$/μm^3) was determined as the number of pores connected with each other divided by the VOI and solid surface to volume ratio (SV, $\times 10^{-3}$/μm) as the ratio of surface area to the volume occupied by the solid within the VOI.

2.7. Statistical analysis

Principle component analyses (PCA; Martens and Martens, 2001) was applied to assess the correlation between the main data variables. The experimental data were fitted to a Scheffe special cubic model (Cornell, 2011).

$$y = \beta_1 x_1 + \beta_2 x_2 + \beta_3 x_3 + \beta_{12} x_1 x_2 + \beta_{13} x_1 x_3 + \beta_{23} x_2 x_3 + \beta_{123} x_1 x_2 x_3 \quad (2)$$

In the model, y is the estimated response. The β's describe the shape of the response surface over the simplex region where β_i is the expected response to the pure component i, β_{ij} is the quadratic coefficient of the binary synergism or antagonism (if β_{ij} is negative) for component i and j, and β_{ijk} represents the ternary blending coefficient of component i, j, k in the interior of the triangle. The PCA was performed using Unscrambler v.10.4.1 (Camo, Oslo, Norway) on mean centered and standardized variables, and the multivariate data modelling using Design-Expert v10 (Stat-Ease, Inc. Minneapolis, USA). The quality of models was assessed by F-statistics, coefficient of multiple determinations (R^2) and lack of fit.

3. Results and discussion

3.1. Data overview

The RheoArt test trials were based on the ingredient mixture design variables, SPC, FPC and water, and a constant shear rate of 300 s^{-1} through the capillary die for apparent viscosity measurements. Starch and protein ingredients show pseudoplastic behavior (shear thinning) fitted to the power law model. However, near parallel shear vs. viscosity lines (log-log plot) have been reported for maize starch at 110 °C in the moisture range of 21–33% (Vergnes and Villemaire, 1987) and soya protein isolate at 120 °C in the moisture range of 25–45% (Bengoechea et al., 2007). This study was based on blends relevant to the fish feed manufacturing industry (Table 2). Possible ingredient interactions with influence on shear tinning effects cannot be excluded based on this study. Other factorial designs are needed to elucidate such effects, however, outside the scope of this study.

The experimental setup resulted in a large span in the measured viscosity and extrudate responses and different extrudate microstructure (Tables 3 and 4 and Fig. 2). The PCA loading plot gives a map of the dominant structure of the design and response variables with principal component 1 (PC-1) explaining 65% and PC-2 22% of the variance (Fig. 3). Effects of SPC and FPC were mainly explained by PC-1, and effects of water by PC-2. SPC was positively associated with apparent viscosity, SEI, open and total porosity, connectivity density
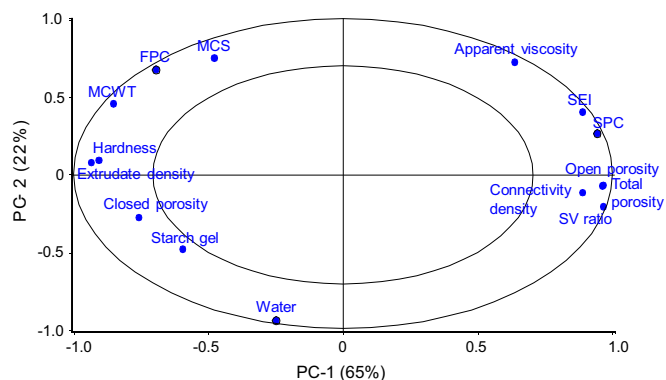

Fig. 3. Principle component analysis (PCA) correlation loading plot based on experimental design and response variables. The two ellipses represent 50 and 100% of explained variance. Abbreviations are explained in Tables 3 and 4.

and solid SV ratio, and negatively associated with hardness, extrudate density, MCWT, close porosity and degree of starch gelatinization. SPC explained 62%, 96% and 84% of the variance in apparent viscosity, SEI and extrudate density, respectively. Comparable correlations between SPC concentration in feed mixes, die apparent viscosity and extrudate SEI and bulk density were documented in the study of Samuelsen et al. (2018) based on twin-screw extrusion.

The FPC showed a positive association with hardness, extrudate density, MCWT and MCS, and a negative association with open and total porosity, connectivity density and solid SV ratio. Water was negatively associated with apparent viscosity and SEI. Water showed, however, poor association with the other response variables (Fig. 3). Apparent viscosity showed a positive correlation with SEI ($R^2 = 0.696$) and a negative correlation to the degree of starch gelatinization ($R^2 = 0.555$). Hardness was positively correlated to extrudate density and MCWT ($R^2 = 0.643$ and 0.668, respectively) and negatively correlated with open and total porosity, connectivity density and SEI ($R^2 = 0.562$ to 0.873). A positive effect of increased density and reduced expansion on hardness are in agreement with studies performed on extruded food foams and fish feed (Hayter et al., 1986; Sørensen, 2012). The highly correlated total and open porosity ($R^2 = 0.970$) were on average 42.2 ± 4.6% and 41.6 ± 4.9% of the total VOI, respectively. Closed pores amounted to only 0.50 ± 0.18% of the total VOI, i.e. most of the pore volume was open. These findings are in line with porosity data found for extruded food and feed products (Bhatnagar and Hanna, 1997; Draganovic et al., 2013). The above results show that RheoArt can be a useful analytical tool giving information about
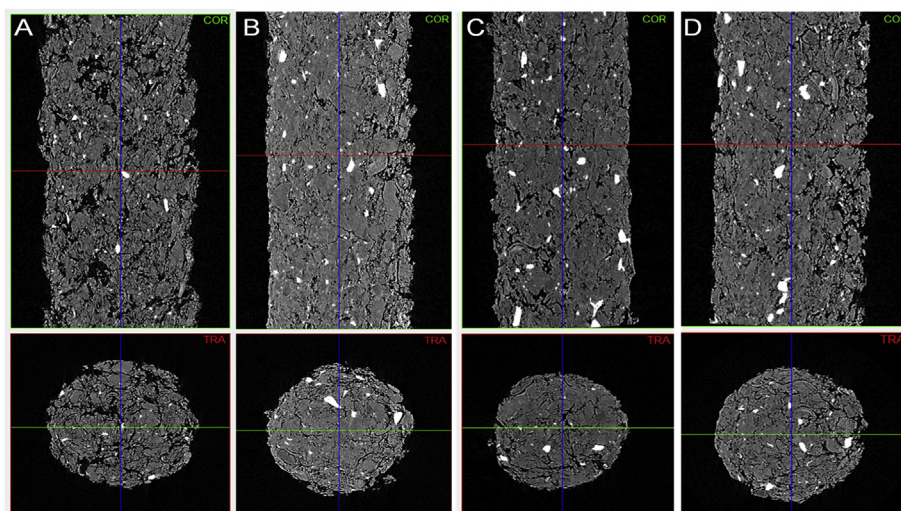

Fig. 2. X-ray microtomography images of extrudate samples in longitudinal (top) and radial (bottom) views. A) Maximum SPC blend concentration (EX1), B) Maximum FPC blend concentration (EX2), C) Maximum water blend concentration (EX3), D) centroid (EX7). Black correspond to air, grey to solid structure, and white to embedded fish bone fragments from fishmeal. Detailed composition data and abbreviations are given in Table 3.

Table 5
Mixture models for the response variables based on pseudo components.

Variables	Models	P - values	Lack of fit (P)	R^2
Apparent viscosity[a]	1384.0 A + 861.0 B + 400.4 C–398.5 AB – 893.9 AC – 201.8 BC	< 0.0001	0.085	0.998
Starch gel[b]	83.1 A + 89.8 B + 92.6 C	0.078	0.368	0.340
Hardness[b]	148.4 A + 252.6 B + 211.9 C	0.0032	0.169	0.703
SEI[b]	1.45 A + 1.17 B + 1.11 C	< 0.0001	0.206	0.972
Extrudate density[b]	893.9 A + 1082.1 B + 1016.7 C	< 0.0001	0.577	0.933
Close porosity[a]	0.25 A + 0.56 B + 0.80 C + 0.46 AB – 0.92 AC – 0.04 BC	0.0165	0.895	0.794
Open porosity[b]	50.6 A + 35.1 B + 40.0 C	0.0004	0.387	0.820
Total porosity[b]	50.7 A + 35.5 B + 40.4 C	0.0005	0.367	0.811
Solid SV ratio[b]	98.1 A + 46.7 B + 70.8 C	0.0002	0.238	0.852
MCWT[a]	33.6 A + 57.8 B + 36.3 C–4.5 AB + 19.0 AC + 23.7 BC	0.0008	0.224	0.941
MCS[b]	134.6 A + 149.5 B + 131.0 C	0.0196	0.217	0.582
Connectivity density[b]	144.1 A + 61.4 B + 95.1 C	0.0118	0.698	0.588

A = soy protein concentrate (SPC), B = fish protein concentrate (FPC), C = water.
Units and abbreviations are explained in Table 4.
  [a] Quadratic model.
  [b] Linear model.

rheological behavior, product physical quality and microstructure relevant to extrusion cooking.

3.2. Impact of the mixture design variables on apparent viscosity and degree of starch gelatinization

Based on 3-component mixture design (Table 3), a quadratic model with high explained variance for apparent viscosity was established (R^2 = 0.998, P < 0.0001; Table 5). The degree of starch gelatinization was fitted to a linear model; however, the model was insignificant with low explained variance (R^2 = 0.340, P = 0.078; Table 5). The mixture design models for apparent viscosity and degree of starch gelatinization showed insignificant lack of fit and no outliers were detected. A low variation of the degree of starch gelatinization was observed for the blends (range 86–92%) except for the maximum SPC blend which had a value of 79% (EX1; Table 4). The weak model may be result of low variance and high measurement uncertainty for the analytical method (± 4.5% at a starch gelatinization level of 96%; Samuelsen and Oterhals, 2016). An alternative method to study the degree of starch gelatinization is differential scanning calorimetry, however, due to the low starch content (82–83 g/kg; Table 2) and multicomponent system a more correct quantification of degree of starch gelatinization in the extrudates may be difficult to obtain (Kraugerud and Svihus, 2011). The highest value for apparent viscosity and the lowest degree of starch gelatinization were found for the maximum SPC blend (Fig. 4A–B). There was a decrease in apparent viscosity when SPC was replaced with FPC and/or water with a higher reduction effect of water than FPC (Fig. 4A). This may be attributed to the much lower viscosity of water compared to FPC and differences in biopolymer interaction, also observed for fishmeal water solubles in the study of Samuelsen and Oterhals (2016) based on twin-screw extrusion trials. The used FPC contains 665 g/kg DM water soluble protein where 61% is free amino acids (< 200 Da) and 81% with molecular weight less than 500 Da, components with a documented plasticizing effect (Ahmad et al., 2018; Oterhals and Samuelsen, 2015). FPC also contains NaCl and fat (Table 1). The fat content was standardized to an equal concentration in this study and NaCl is reported to have insignificant plasticizing effect on SPC (Ahmad et al., 2018). The temperature and capillary die shear rate and diameter were kept constant in this study. The observed viscosity reduction with increased concentration of FPC and/or water reflects a higher effect of temperature on viscosity reduction in the rubbery phase, confirming a plasticizing effect of these constituents. The observed lower degree of starch gelatinization for the maximum SPC blend may be due to incomplete hydration and gelatinization of the starch molecules.

Tan et al. (2008) reported viscosity increase during starch

gelatinization due to granule swelling and Samuelsen et al. (2013) observed a positive correlation between the degree of starch gelatinization and viscosity increase in the extruder barrel. These results could not be confirmed in this study, probably caused by a dominating effect of the mixture components and with highest viscosity found for the maximum SPC blend.

3.3. Impact of the mixture design variables on extrudate hardness

Hardness is an important physical quality parameter for fish feed (Sørensen, 2012). The measured values ranged from 136.2 to 244.5 N, which are comparable to the range reported for dried uncoated extruded fish feed pellet high in SPC (Samuelsen et al., 2018). Hardness was fitted to a linear model (R^2 = 0.703, P = 0.003; Table 5). The model showed insignificant lack of fit and no outliers were detected. The lowest value of hardness was found on the vertex of the maximum SPC blend (Table 4, Fig. 4C) and may be attributed to insufficient concentration of water and/or FPC. The RheoArt processing parameters were constant and it can be hypothesized that at the low moisture content (200 g/kg) and no FPC addition, the achieved thermomechanical treatment was insufficient for complete plasticization. This may have resulted in a heterogeneous product consisting of dispersed particles reducing the network formation and extrudate hardness (Areas, 1992; Mitchell and Areas, 1992; Samuelsen et al., 2018).

Increased concentration of both FPC and water increased extrudate hardness. However, the effect of FPC was higher compared to water (Fig. 4C). In contrast to water, FPC will be carried over to the dried extrudate and reduce the need for water removal in the drier. This will give less pore structure, denser pellet and increased hardness. The increase in peptides and amino acids in the dried extrudate will also contribute to intermolecular binding network by hydrogen and ionic bond interactions (Samuelsen et al., 2013; Samuelsen and Oterhals, 2016).

3.4. Impact of the mixture design variables on SEI and extrudate density

The expansion parameters, SEI and extrudate density were fitted to linear models with high explained variance (R^2 = 0.972 and 0.933, respectively, P < 0.0001; Table 5). The models showed insignificant lack of fit and no outliers were detected. The maximum SPC blend produced the extrudate with the highest value for SEI and the lowest value for extrudate density (Fig. 4D–E). Increased concentration of both FPC and water resulted in decreased SEI and increased extrudate density. The effect of FPC was slightly lower on SEI and significantly higher on extrudate density compare to water. Several studies have explained the mechanism of expansion as a combination of bubble growth and
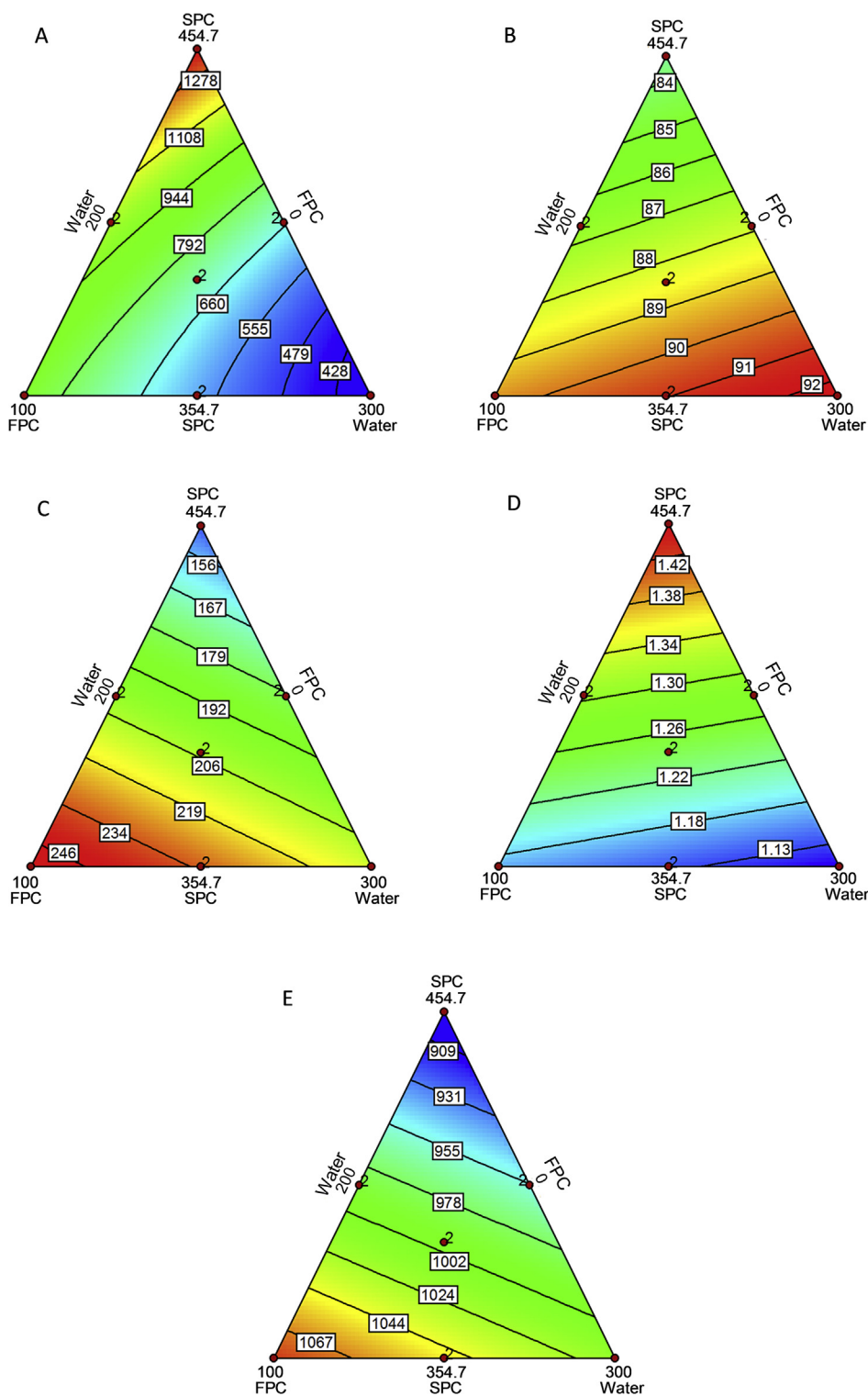
Fig. 4. Contour plots for apparent viscosity and extrudate response variables. Actual inclusion levels of SPC (g FFDM kg^{-1}), FPC (g FFDM kg^{-1}) and water (g kg^{-1}) are given for pure (vertex) and binary (edge) points. The contours are flagged with the actual units of the respective response. Solid red circles represent the design points. A) Apparent viscosity (Pa s), B) Degree of starch gelatinization (% of total starch), C) Hardness (N), D) Sectional expansion index, E) Extrudate density (kg/m^3). Detailed composition data and abbreviations are given in Table 3. (For interpretation of the references to colour in this figure legend, the reader is referred to the Web version of this article.)

shrinkage in correlation with phase transition, degree of transformation and fluid viscosity behind and after the die exit (Della Valle et al., 1997; Fan et al., 1994; Moraru and Kokini, 2003; Strahm et al., 2000). The temperature behind the die was kept constant in this study; i.e. the main driving force for steam vaporization is equal (Fan et al., 1994). The observed high expansion for SPC rich blends may be due to reduced degree of plasticization and weak intermolecular interactions holding the structure together during steam flash off. This have led to the observed expanded and fragile extrudate structure (Table 4; Fig. 2A).

The observed decreasing SEI and extrudate density with increasing

concentration of either FPC or water may be linked to increased plasticization and intermolecular binding forces contributing to the formation of denser pellet with a smoother outer surface as shown in XMT images (Fig. 2B and C).

3.5. Impact of the mixture design variables on 3-dimensional cellular structure

The microstructure response models had high degree of explained variance with R^2 = 0.582 to 0.941 and P = 0.0165 to 0.0002 (Table 5).
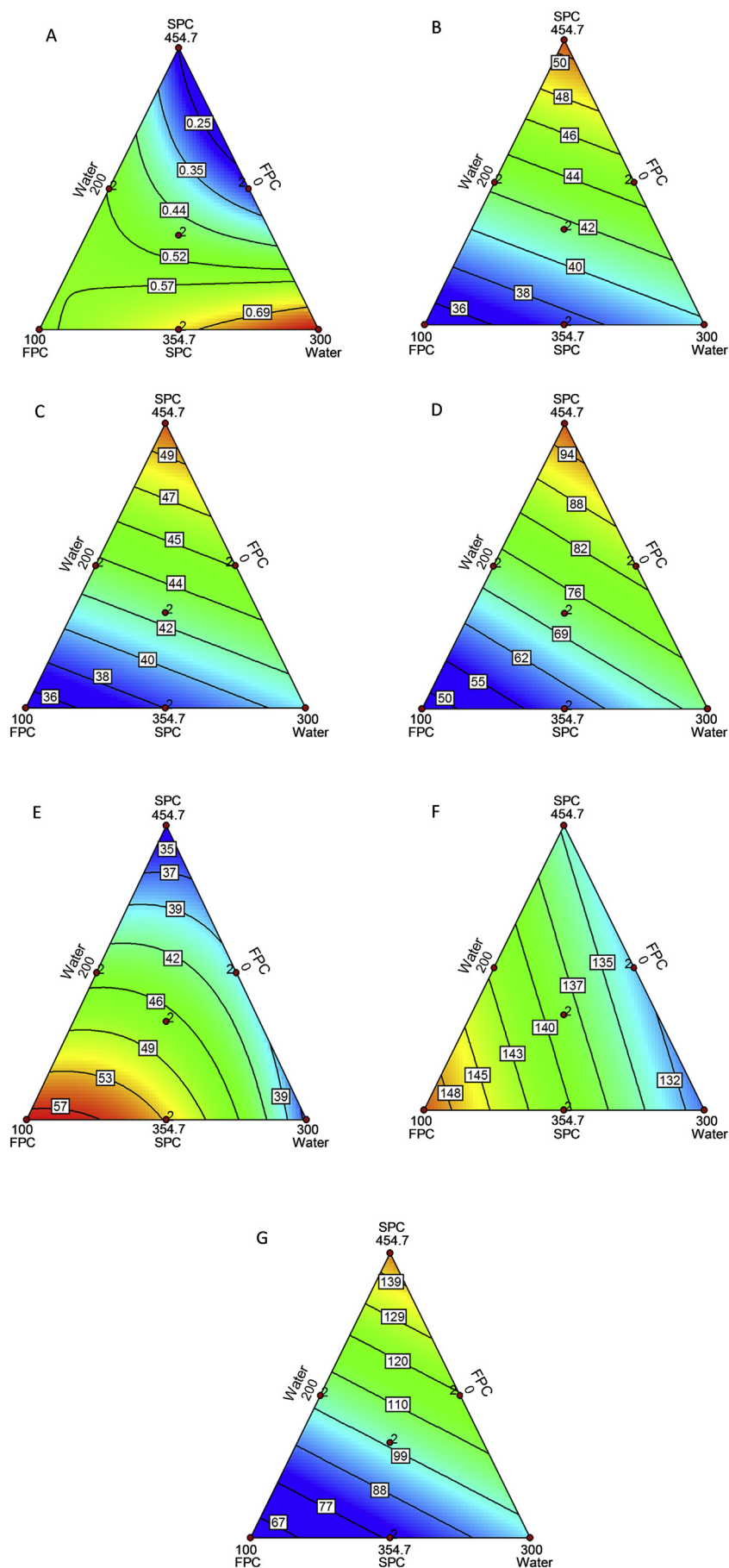
Fig. 5. Contour plots for microstructure response variables. Actual inclusion levels of SPC (g FFDM kg^{-1}), FPC (g FFDM kg^{-1}) and water (g kg^{-1}) are given for pure (vertex) and binary (edge) points. The contours are flagged with the actual units of the respective response. Solid red circles represent the design points. A) Closed porosity (%), B) Open porosity (%), C) Total porosity (%), D) solid SV ratio (10^{-3}/μm), E) MCWT (μm), F) MCS (μm), G) Connectivity density ($\times 10^{-7}$/μm^3). Detailed composition data and abbreviations are given in Tables 3 and 4 (For interpretation of the references to colour in this figure legend, the reader is referred to the Web version of this article.)

The models showed insignificant lack of fit and no outliers were detected except for MCS, where one outlier (EX4) was removed to improve model fit and predicting power. EX4 was identified by the modelling software as an outlier based on a high residual value. EX11 is a true replicate of EX4 (Table 4) and fit well with the MCS regression model. A quadratic model was established for close porosity. The lowest value was found on the vertex of the maximum SPC blend and are increasing with both FPC and water addition (Fig. 5A). The closed pores amounted to only 0.50 ± 0.18% of the total VOI. Open porosity, total porosity, and solid SV ratio were fitted to linear models with the highest value found on the vertex of the maximum SPC blend and the lowest value on the maximum FPC blend (Fig. 5B–D). A quadratic model and a linear model were established for MCWT and MCS, respectively. Samples high in FPC showed the highest values and samples high in SPC the lowest values of both MCWT and MCS (Fig. 5E–F). Connectivity density was fitted to linear model with the highest value found on the vertices of the maximum SPC blend and the lowest value on the on the vertices of the maximum FPC blend (Fig. 5G). The cell size-volumetric and cell wall thickness-volumetric distribution curves are found in Fig. 6A–B. The cell size-volumetric distribution showed two distinct peaks with small cell sizes (range of 5–64 μm) comprising 56%, 41%, 51% and 47% of the total pore volume for the maximum SPC blend, maximum FPC blend, maximum water blend and centroid, respectively. In the larger size range (297–381 μm), the maximum SPC blend was deviating from the others with a distribution in the 371–381 μm range which make up 18% of the total pore volume. Visually from Fig. 2A, the large pores were unevenly distributed over the whole sample mass. The maximum FPC blend and maximum water blend showed comparatively equal volume (23.5 ± 1.8%) but FPC had slightly larger pore sizes (FPC = 307–312 μm; water = 297–302 μm; Fig. 6A). Visually, from Fig. 2B, the larger pores were mostly located on the surface and with a denser structure in the middle for the maximum FPC blend. For water (Fig. 2C) the larger pores were more evenly distributed. Cell wall thickness distribution ranged between 5 and 154 μm where SPC showed the narrowest range and FPC the broadest range. There were positive correlations between SEI and the microstructural properties total and open pores, solid SV ratio and connective density (Fig. 3). Hardness and extruded density were negatively correlated with the same properties. All above responses were also fitted to linear models (Table 5). Both hardness and extrudate density were positive correlated with MCWT (Fig. 3). The findings confirm that extrudate hardness and expansion were explained by the extrudate microstructure and in line with other studies (Bhatnagar and Hanna, 1997; Agbisit et al., 2007; Robin et al., 2010). However, the achieved thermomechanical transformation and degree of cell-wall homogeneity may also influence these properties.

3.6. Industrial applications

For high energy fish feed most of the oil is added in a post extrusion vacuum coating operation (Strauch, 2005). Oil adsorption and leakage are directly linked to pellet microstructure (Moreira et al., 1997; Draganovic et al., 2013; Dethlefsen, 2017). Highest values of the structure parameters open porosity, pores size and connectivity density were found for samples high in SPC and will thereby favor oil adsorption. However, these parameters will also increase the oil leakage due to lower capillary pressure (Dethlefsen, 2017; Samuelsen et al., 2018). The microstructure measured for samples plasticized by water (Fig. 5B–G) may give favorable conditions for increased oil adsorption and reduced leakage compared to the samples plasticized by FPC. However, the extrudate hardness were lower for the water plasticized samples (Fig. 4C). The RheoArt measurements were performed under standardized conditions and the SPC blend plasticized with FPC gave different extrudate properties compared to water plasticization. However, FPC added at a concentration of 65–70 g FFDM/kg gave values of hardness, extrudate density, open and total porosity, SV ratio and connectivity density similar to SPC added 100 g/kg of water (Fig. 4C
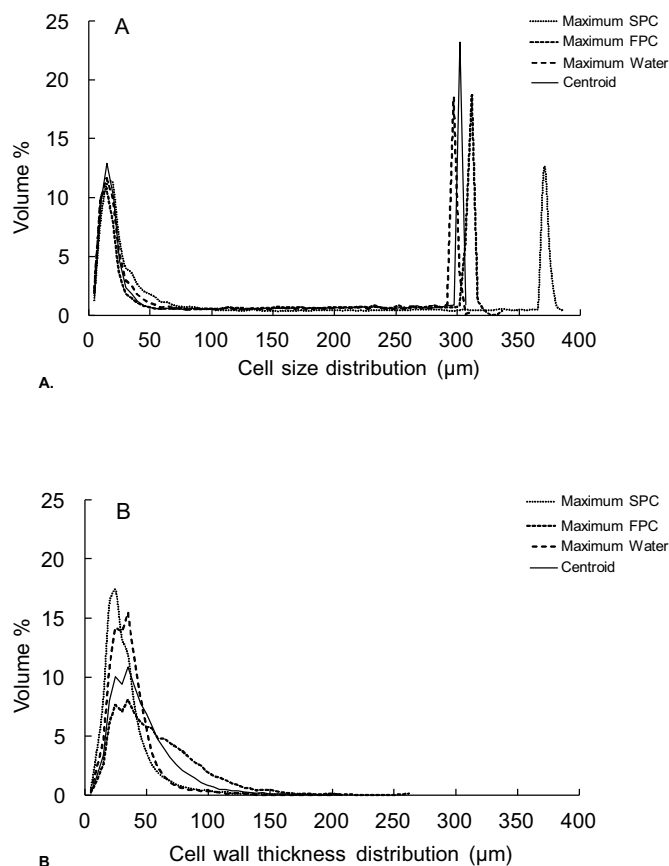

Fig. 6. A. Cell size-volumetric distribution for the blend with maximum soy protein concentrate (SPC; EX1), maximum fish protein concentrate (FPC; EX2), maximum water (EX3) and the centroid (EX7). B. Cell wall thickness-volumetric distribution for the blend with maximum soy protein concentrate (SPC; EX1), maximum fish protein concentrate (FPC; EX2), maximum water (EX3) and the centroid (EX7).

and E; Fig. 5B–D and G). This demonstrate that FPC can partly replace water as plasticizer in feed mixes without compromising pellet physical quality, oil adsorption and leakage.

4. Conclusion

The pre-shearing capillary rheometer RheoArt enables plasticization of the sample material prior to rheological and physical measurements relevant to extrusion cooking. The ratio between the components SPC, FPC and water in the studied mixture design had significant impact on the measured apparent viscosity, extrudate hardness, expansion parameters and microstructure. Extrudate physical properties and expansion were described by the extrudate microstructure (porosity, pores size distribution, cell wall thickness and distribution) assessed by X-ray microtomography. The findings document that X-ray microtomography can be a useful tool for the feed manufacturing industry to better understand how to modulate and control physical pellet quality, oil adsorption in the post extrusion vacuum coating operation, and leakage. SPC blend plasticized with FPC gave different extrudate properties compared to water plasticization. FPC added at a concentration of 65–70 g FFDM/kg gave values of hardness, extrudate density and microstructure comparable to SPC added 100 g/kg of water, confirming the potential for the use of FPC as a plasticizer and binder in the fish feed extrusion process.

Acknowledgements

References

Agbisit, R., Alavi, S., Cheng, E.Z., Herald, T., Trater, A., 2007. Relationships between microstructure and mechanical properties of cellular cornstarch extrudates. J. Texture Stud. 38, 199–219.

Ahmad, R., Samuelsen, T.A., Garvik, A.B., Oterhals, Å., 2018. Effect of amino acid, pH and mineral salts on glass transition and flow behavior of soy protein concentrate. Int. J. Food Sci. Technol. 53, 1425–1433.

AOAC, 2000. Official Methods of Analysis, sixteenth ed. Association of Official Analytical Chemistry, Gaithersburg, MD Official Method 937.09.

Areas, J.A.G., 1992. Extrusion of food proteins. Crit. Rev. Food Sci. Nutr. 32, 365–392.

Barron, C., Buleon, A., Colonna, P., Della Valle, G., 2000. Structural modifications of low hydrated pea starch subjected to high thermomechanical processing. Carbohydr. Polym. 43, 171–181.

Bengoechea, C., Arrachid, A., Guerrero, A., Hill, S.E., Mitchell, J.R., 2007. Relationship between the glass transition temperature and the melt flow behavior for gluten, casein and soya. J. Cereal Sci. 45, 275–284.

Bhatnagar, S., Hanna, M.A., 1997. Modification of microstructure of starch extruded with selected lipids. Starch Staerke 49, 12–20.

Bligh, E.G., Dyer, W.J., 1959. A rapid method of total lipid extraction and purification. Can. J. Biochem. Physiol. 37, 911–917.

Chiang, B.Y., Johnson, J.A., 1977. Measurement of total and gelatinized starch by glucoamylase and omilron-toluidine reagent. Cereal Chem. 54, 429–435.

Cornell, J.A., 2011. A Primer on Experiments with Mixtures. Response Surface Methodology. John Wiley & Sons, Inc., Hoboken, New Jersey.

Della Valle, G., Vergnes, B., Colonna, P., Patria, A., 1997. Relations between rheological properties of molten starches and their expansion behaviour in extrusion. J. Food Eng. 31, 277–295.

Dethlefsen, M.W., 2017. Die Hard - improving the physical quality of extruded fish feed pellets. Kgs. Lyngby: National Food Institute, Technical University of Denmark 52 p.

Draganovic, V., van der Goot, A.J., Boom, R., Jonkers, J., 2011. Assessment of the effects of fish meal, wheat gluten, soy protein concentrate and feed moisture on extruder system parameters and the technical quality of fish feed. Anim. Feed Sci. Technol. 165, 238–250.

Draganovic, V., Van der Goot, A.J., Boom, R., Jonkers, J., 2013. Wheat gluten in extruded fish feed: effects on morphology and on physical and functional properties. Aquacult. Nutr. 19, 845–859.

Fan, J.T., Mitchell, J.R., Blanshard, J.M.V., 1994. A computer-simulation of the dynamics of bubble-growth and shrinkage during extrudate expansion. J. Food Eng. 23, 337–356.

Glencross, B., Hawkins, W., Maas, R., Karopoulos, M., Hauler, R., 2010. Evaluation of the influence of different species and cultivars of lupin kernel meal on the extrusion process, pellet properties and viscosity parameters of salmonid feeds. Aquacult. Nutr. 16, 13–24.

Hayter, A.L., Smith, A.C., Richmond, P., 1986. The physical-properties of extruded food foams. J. Mater. Sci. 21, 3729–3736.

ISO 5983, 2009. Animal Feeding Stuffs (Part 2) – Determination of Nitrogen Content and Calculation of Crude Protein Content: Block Digestion/Steam Distillation Method. International Organization for Standardization, Geneva, Switzerland.

ISO 5984, 2002. Animal Feeding Stuffs - Determination of Crude Ash. International Organization for Standardization, Geneva, Switzerland.

ISO 6496, 1999. Animal Feeding Stuffs – Determination of Moisture and Other Volatile Matter Content. International Organization for Standardization, Geneva, Switzerland.

Kraugerud, O.F., Svihus, B., 2011. Tools to determine the degree of starch gelatinization in commercial extruded salmon feeds. J. World Aquacult. Soc. 42, 914–920.

Kraugerud, O.F., Jorgensen, H.Y., Svihus, B., 2011. Physical properties of extruded fish feed with inclusion of different plant (legumes, oilseeds, or cereals) meals. Anim. Feed Sci. Technol. 163, 244–254.

Landis, E.N., Keane, D.T., 2010. X-ray microtomography. Mater. Char. 61, 1305–1316.

Martens, H., Martens, M., 2001. Multivariate Analysis of Quality. An Introduction. John Wiley & Sons Ltd, West Sussex, UK, pp. 466.

Mitchell, J.R., Arêas, J.A.G., 1992. Structural changes in biopolymers during extrusion. In: Kokini, J.L., Ho, C.-T., Karwe, M.V. (Eds.), Food Extrusion Science and Technology. Marcel Dekker Inc., New York, NY, pp. 345–360.

Moraru, C.I., Kokini, J.L., 2003. Nucleation and expansion during extrusion and microwave heating of cereal foods. Compr. Rev. Food Sci. Food Saf. 2, 147–165.

Moreira, R.G., Sun, X.Z., Chen, Y.H., 1997. Factors affecting oil uptake in tortilla chips in deep-fat frying. J. Food Eng. 31, 485–498.

Nunez, M., Della Valle, G., Sandoval, A.J., 2010. Shear and elongational viscosities of a complex starchy formulation for extrusion cooking. Food Res. Int. 43, 2093–2100.

Oterhals, Å., Samuelsen, T.A., 2015. Plasticization effect of solubles in fishmeal. Food Res. Int. 69, 313–321.

Robin, F., Engmann, J., Pineau, N., Chanvrier, H., Bovet, N., Della Valle, G., 2010. Extrusion, structure and mechanical properties of complex starchy foams. J. Food Eng. 98, 19–27.

Samuelsen, T.A., Oterhals, Å., 2016. Water-soluble protein level in fishmeal affects extrusion behaviour, phase transitions and physical quality of feed. Aquacult. Nutr. 22, 120–133.

Samuelsen, T.A., Mjøs, S.A., Oterhals, Å., 2013. Impact of variability in fishmeal physicochemical properties on the extrusion process, starch gelatinization and pellet durability and hardness. Anim. Feed Sci. Technol. 179, 77–84.

Samuelsen, T.A., Oterhals, Å., Kousoulaki, K., 2018. High lipid microalgae (*Schizochytrium sp.*) inclusion as a sustainable source of n-3 long-chain PUFA in fish feed-Effects on the extrusion process and physical pellet quality. Anim. Feed Sci. Technol. 236, 14–28.

Sikorski, Z.E., Gildberg, A., Ruiter, A., 1995. Fish products. In: Ruiter, A. (Ed.), Fish and Fishery Products, Composition, Nutritive Properties and Stability. CAB International, Wallingford, UK, pp. 315–345.

Sørensen, M., 2012. A review of the effects of ingredient composition and processing conditions on the physical qualities of extruded high-energy fish feed as measured by prevailing methods. Aquacult. Nutr. 18, 233–248.

Sørensen, M., Berge, G.M., Thomassen, M., Ruyter, B., Hatlen, B., Ytrestøyl, T., Aas, T.S., Åsgård, T., 2011. Today's and Tomorrow's Feed Ingredients in Norwegian aquaculture. Nofima report 52/2011. 978-82-7251-943-7.

Strahm, B., Plattner, B., Huber, G., Rokey, G., 2000. Application of food polymer science and capillary rheometry in evaluating complex extruded products. Cereal Foods World 45, 300–302.

Strauch, W., 2005. Einflussgrößen beim vakuumcoating zur herstellung energiereicher mischfutter. Muhle + Mischfuttertechnik 142, 97–103.

Tan, I., Torley, P.J., Halley, P.J., 2008. Combined rheological and optical investigation of maize, barley and wheat starch gelatinization. Carbohydr. Polym. 72, 272–286.

Trater, A.M., Alavi, S., Rizvi, S.S.H., 2005. Use of non-invasive X-ray microtomography for characterizing microstructure of extruded biopolymer foams. Food Res. Int. 38, 709–719.

Vergnes, B., Villemaire, J.P., 1987. Rheological behaviour of low moisture molten maize starch. Rheol. Acta 26, 570–576.

Ytrestøyl, T., Aas, T.S., Asgard, T., 2015. Utilisation of feed resources in production of Atlantic salmon (Salmo salar) in Norway. Aquaculture 448, 365–374.